Published in final edited form as:
Am J Physiol Regul Integr Comp Physiol. 2005 October ; 289(4): R1155–R1168.

P2X2 and P2X3 Receptor Expression in Postnatal and Adult Rat Urinary Bladder and Lumbosacral Spinal Cord

Simon Studeny[1], **Ali Torabi**[1], and **Margaret A. Vizzard**[1,2]

[1]*Department of Neurology, Anatomy and* [2]*Neurobiology, University of Vermont, College of Medicine, Burlington, Vermont, VT 05405*

Abstract

P2X receptors mediate the effects of ATP in micturition and nociception. During postnatal maturation, a spinobulbospinal reflex and voluntary voiding replace primitive voiding reflexes. This may involve changes in neuroactive compounds and receptors in bladder reflex pathways. We examined P2X2 and P2X3 receptors in bladder and spinal cord from postnatal (P0-P36) and adult Wistar rats. Western blot of whole bladders for P2X2 and P2X3 expression was performed. Immunostaining for P2X2 and P2X3 receptors in urothelium and detrusor smooth muscle whole-mounts and spinal cord sections was examined. Western blot demonstrated an age-dependent decrease (R^2= 0.96, $p \leq 0.005$) in P2X2 receptor expression in bladder whereas P2X3 receptor expression in bladder peaked ($p \leq 0.005$) from P14-P21. P2X2-immunoreactivity (IR) was present in urothelial cells, suburothelial plexus, detrusor smooth muscle and serosa at birth with staining in urothelial cells and serosa being most predominant. With increasing postnatal age, the intensity of P2X2-IR decreased in urothelial cells but increased in suburothelial plexus. P2X3-IR increased in urothelial cells and suburothelial plexus with postnatal age whereas staining in detrusor and serosa remained relatively constant. At birth, P2X3-IR was present in the dorsal horn (DH), lateral collateral pathway (LCP), and dorsal commissure. With increasing age, P2X3-IR was restricted to superficial DH and LCP. P2X2-IR was present in ependyme cells (S-100-IR) of the central canal as early as P2. These studies demonstrate plastic expression of P2X2 and P2X3 receptors in bladder and spinal cord during early postnatal development at times coincident with appearance of mature voiding patterns.

Keywords

postnatal development; micturition reflexes; sacral parasympathetic nucleus; dorsal commissure; dorsal horn

Introduction

The neural control of micturition undergoes marked changes during early postnatal development (11,14,31,48,49). In newborn rats and cats, micturition is dependent upon a spinal reflex pathway that is activated when the mother licks the perineal region of the young animal (perineal-to-bladder reflex) (15,16,49). This reflex pathway consists of a somatic afferent limb in the pudendal nerve and a parasympathetic efferent limb in the pelvic nerve. These afferents induce a bladder contraction and coordinated urethral sphincter activity resulting in complete

Contact Information: Margaret A. Vizzard, Ph.D., University of Vermont College of Medicine, Department of Neurology, D415A Given Research Building, Burlington, VT 05405, Phone: 802-656-3209, Fax: 802-656-8704, Email: margaret.vizzard@uvm.edu.

Grants
This work was funded by NIH grants DK051369, DK060481, DK065989, NS040796.

bladder emptying (29). During postnatal maturation, primitive reflex pathways organized at the spinal level are replaced by a spinobulbospinal reflex leading to emergence of voluntary voiding (12,13). The manner in which this is accomplished is not known but it is suggested that postnatal maturation of voiding function involves prominent reorganization of synaptic connections in bladder reflex pathways. This reorganization leads to downregulation of primitive spinal mechanisms and upregulation of mature supraspinal pathways (12,13). Previous studies have suggested the importance of neuroactive compounds in the process of maturation of the micturition reflexes during prenatal and early postnatal development (19, 26,41).

There is a substantial body of literature that supports a functional role for adenosine triphosphate (ATP) in the modality of mechanotransduction in the urinary bladder (7,57). ATP can be produced and released from the urothelium in response to stretch (21,45,46) and this release can be augmented in urothelial cells from patients with interstitial cystitis (IC)(45) and benign prostatic hyperplasia (46). There are seven subtypes of purinergic (P)2X-ATP receptors (37) and recent studies have demonstrated that bladder afferent cells in the L6-S1 DRG express predominantly P2X2/3 heteromeric receptors (57). In addition, P2X3-immunoreactive nerve fibers in the suburothelial plexus of the bladder have been demonstrated (10,53). Upregulation of P2X3 receptors has also been demonstrated in cultured urothelial cells from patients with IC during in vitro stretch (44). Upregulation of P2X2 receptors in detrusor smooth muscle from patients with idiopathic detrusor instability has also been demonstrated (38). P2X3 receptor knockout mice exhibit bladder hyporeflexia on cystometry with decreased voiding frequency and increased bladder capacity and voided volume but normal bladder pressures (10). Thus, P2X2 and P2X3 receptors may play unique, tissue specific roles in micturition reflex pathways and receptor expression can be altered by urinary bladder dysfunction.

Although the ontogeny of P2X3 receptors in mouse DRG has been described (40), no studies have examined the developmental expression of P2X2 or P2X3 receptors in the rat urinary bladder or lumbosacral spinal cord. The ontogeny of responses to purines in postnatal and adult rat bladder have been examined (8,25,32,36) with differences in potency to ATP being attributed to postnatal changes in receptor number or agonist efficacy (35). A mature voiding reflex that is induced by bladder distension is not functional in neonatal animals (12,15). These studies were performed to determine if P2X2 and/or P2X3 receptor expression is altered during early postnatal development when primitive voiding reflexes are replaced by a mature, spinobulbospinal micturition reflex. The goals of the study were to: (1) determine the expression of P2X2 and P2X3 receptors in whole urinary bladder from postnatal and adult rats by western blot; (2) determine the tissue expression of P2X2 and P2X3 receptors in detrusor smooth muscle and urothelium whole-mounts in postnatal and adult rats; (3) determine the expression of P2X2 and P2X3 receptor in lumbosacral spinal cord from postnatal and adult rats by immunohistochemistry; (4) quantify P2X3 receptor expression in dorsal horn of L6 spinal cord from postnatal and adult rats. Some aspects of this work have been reported in an abstract (43).

Material and Methods

Experimental animals

Rat pups (Charles River, Canada; postnatal day (P)0, P1, P2, P7, P14, P21, P28, P36; n=14 each) and adult rats (P90; n=14) were used for this study. Rat pups were born to timed-pregnant rats and several postnatal ages were studied from each litter born. Developmental ages, prior to (P0-P14) or following (P21-adult) the development of the spinobulbospinal micturition reflex were selected and analyzed (9). In these studies, day of birth is referred to as P0. All experimental protocols involving animal use were approved by the University of Vermont Institutional Animal Care and Use Committee (05–026). Animal care was under supervision

of the University of Vermont Office of Animal Care Management in accordance with the Association for Assessment and Accreditation of Laboratory Animal Care (AAALAC) and National Institutes of Health guidelines.

Tissue harvest

Both male and female rat pups (P0, P2, P7, P14, P21, P28, P36; n=3 each) and female adult rats (P90; n=6) were deeply anesthetized with isoflurane (4%) and then euthanized by decapitation (pups) or thoracotomy (adult rats). Then the urinary bladder was rapidly dissected, weighed and placed in Krebs solution (119.0 mmol NaCl, 4.7 mmol KCl, 24.0 mmol $NaHCO_3$, 1.2 mmol KH_2 PO_4, 1.2 mmol $MgSO_4$, 11.0 mmol glucose, 2.5 mmol $CaCl_2$). The bladder was cut open along the midline and the urothelium was removed as previously described (58). The urothelium and bladder musculature were then processed separately. Urothelium and bladder musculature were cut in half with one half being processed for P2X2-immunoreactivity (IR) and the other half for P2X3-IR by a free-floating technique. Whole rat bladders were harvested as above and used for western blot analysis of P2X2- and P2X3-IR (see below). The spinal cord (cervical to sacral) was removed, placed in paraformaldehyde (4%), segmented (L6-S1), placed in sucrose (20%) for 24 hours and then sectioned (20 μm) in the transverse plane using a cryostat. Spinal cord segments were identified based upon at least two criteria: (1) the T13 dorsal root ganglion (DRG) exits after the last rib and (2) the L6 vertebra is the last moveable vertebrae followed by the fused sacral vertebrae. Another less precise criterion is the observation that the L6 DRG are the smallest ganglia following the largest, L5 DRG. In rat pups younger that P14, segmentation using guidance from DRG, vertebrae and peripheral roots was not possible. Thus, segmentation was based on locating the lumbar enlargement and then estimating the location of the L6-S1 spinal cord caudal to this. This estimation was later confirmed by immunostaining the autonomic nucleus in the L6-S1 spinal segments with neuronal nitric oxide synthase (nNOS)-IR (51)(see below). Spinal cord sections from each animal were processed for P2X2- and P2X3-IR.

Western blot

Urinary Bladder

Whole rat bladders (P0-P2, P3, P7, P14, P21, P28 n = 88 and P63-90 (adult; 150–200 g) n= 11) were homogenized in tissue protein extraction reagent with complete protease inhibitor tablets (Roche, Indianapolis, IN). Aliquots of homogenates were removed for protein assay using the Coomassie Plus Protein Assay Reagent Kit (Pierce). Samples (40 mg) were suspended in sample buffer for fractionation on 10% Tris-glycine gels and subjected to SDS-PAGE under reducing conditions. Proteins were transferred to a nitrocellulose membrane. Efficiency of transfer was evaluated using Ponceau S reagent in 0.05% trichloracetic acid. Membranes were blocked overnight (with shaking at 4°C) in Tris-buffered saline + 0.05% Tween (TBST), 5% nonfat dry milk, and 3% bovine serum albumin. After they were rinsed (3 times X 10 min each) in TBST, membranes were incubated in primary antibody (Table 1) for 2 h at room temperature and then rinsed three times (10 min each with shaking) in TBST. Washed membranes were then incubated in HRP-conjugated donkey anti goat antibody IgG (1:5000, Jackson) for 1 hour at room temperature for enhanced chemiluminescence detection (Pierce). The blot was exposed to Biomax film (Kodak) and developed. Ponceau S (Sigma) staining of the same membrane or western blotting of ERK (New England Biolabs, Beverly, MA) were used as loading controls. Antibody specificity was confirmed with absorption controls. Preabsorption of P2X2 and P2X3 antisera with appropriate immunogen (1 μg ml^{-1}) reduced staining in blots to background levels.

Immunohistochemistry

Urothelium and detrusor whole-mounts were processed for P2X2- and P2X3-immunoreactivity using a free-floating technique (59). Spinal cord tissue was stained using an on-slide processing technique (51). Urothelium, detrusor and spinal cord sections were incubated with primary antibody (Table 1) overnight at room temperature. Slides were then washed (3 x 10 minutes) with 0.1 KPBS, pH 7.4. Tissues were then incubated with species-specific secondary antisera (Table 1) for 2 hours at room temperature. Slides were washed (3 x 10 minutes) with 0.1 KPBS (pH 7.4) and then placed under a coverslip using Citifluor (Citifluor, London, UK). In the absence of primary or secondary antibody, no positive immunostaining for P2X2 or P2X3 was observed. Specificity of antisera was also confirmed by absorption controls. P2X2 antiserum and P2X3 antiserum were preabsorbed with appropriate immunogen (1 μg ml^{-1}) and then applied to tissue sections. Preabsorption reduced staining to background levels. Tissues from several postnatal or adult animals were stained simultaneously.

To determine whether some P2X2-immunoreactive structures in the spinal cord were neurons or glial cells, spinal cord sections were labeled with the pan neuronal marker, HuC/D, the astrocyte marker, glial fibrillary acidic protein (GFAP), or ependyme cell marker (S-100) (Fig. 1). Double-labeling for P2X2-and Hu-IR and P2X2- and GFAP was performed. Double-labeling for P2X2- and S-100 was not possible due to common hosts. P2X2- and P2X3-immunoreactive fibers in the suburothelial plexus and serosa were also stained for protein gene product 9.5 to confirm that the structures were nerve fibers (Table 1). After primary antibody application for Hu, GFAP or S-100, tissues were rinsed and then species-specific secondary antibodies were applied (Table 1) as above.

Antisera Selection and Assessment of Positively Stained Structures

Different P2X2 and P2X3 antisera (Table 1) were used in this study for either western blotting or immunohistochemistry. P2X2 antiserum (Table 1) was successfully used for both applications with changes in concentration. All tissues examined (urothelium, detrusor smooth muscle and spinal cord) exhibited robust staining with low background. In contrast, different P2X3 antisera were used for western blotting or immunohistochemistry because of inconsistent results and high background. Thus, the antisera listed in Table 1 reflect the choices made for western blot or immunohistochemistry in specific tissues (spinal cord vs. bladder). As stated above, P2X-IR resulting from each antisera was successfully blocked by preabsorption with immunogen (1 μg ml^{-1}).

Staining observed in experimental tissue was compared to that observed from experiment-matched negative controls. Structures (cell bodies, smooth muscle, and nerve fibers) exhibiting immunoreactivity that was greater than the background level observed in experiment-matched negative controls were considered positively stained.

Figure preparation and data analysis

Immunohistochemistry, Urinary Bladder

Confocal scanning laser microscopy was used to examine immunostained urothelium and bladder detrusor from all ages with Bio-Rad MCR 1024 ES confocal scanning microscopy system (Bio-Rad Laboratories, Hercules, CA, USA). For each z-axis interval (1–2 μm), tissue sections are Kalman scanned three times using Krypton-argon laser with specific excitation wavelengths and sequential images are captured for sequential computer-generated overlay and analysis. Immunostaining with P2X2 and P2X3 antibodies were visualized with an excitation wavelength of 647 nm for Cy3-conjugated secondary antibodies. Images were captured with the use of a 60x objective lens (1024 x1024 pixel, 8-bit grayscale format).

Sections were also examined under an Olympus fluorescence photomicroscope (model BX51, Optical Analysis Corp., Nashua, NH). Cy3 was visualized with a filter with an excitation range of 560–596 nm and an emission range from 610–655 nm. Cy2 was visualized with a filter with an excitation range of 470 nm and emission range at 525nm. In all cases, both the urothelium and detrusor smooth muscle whole-mounts were examined for P2X2 and P2X3 receptor staining. For structures with a known differential distribution (i.e. suburothelial plexus) (1), images were captured from bladder regions with the densest P2X2 and P2X3 receptor staining.

Immunohistochemistry, Spinal Cord

Tissues were examined under an Olympus fluorescence photomicroscope for visualization of Cy3. Cy3 was visualized with a filter with an excitation range of 560–596 nm and an emission range from 610 to 655 nm. Intensity of P2X3 IR in DH was quantified using MetaMorph Image Analysis software (Universal Imaging, West Chester, PA, USA). Three identical areas (30 x 30 μm) were chosen (medial, lateral and intermediate aspect of dorsal horn (DH) and staining intensity in these areas was thresholded, quantified and averaged per tissue section. This measurement was performed on three animals from six randomly selected tissue sections per animal. For all pictures and quantification, the threshold remained constant. P2X3-IR nerve fibers in the DH exceeding threshold were summarized and expressed in percentage (%) of DH expressing P2X3-IR. Comparisons of P2X3 staining in the DH at all ages were performed using analysis of variance. Percentage data were arcsin transformed to meet the requirements of this statistical test. Animals, processed and analyzed on the same day, were tested as a block in the analysis of variance. Two variables were being tested in the analysis: (1) age and (2) the effect of day (i.e., tissue from different postnatal or adult groups of animals were processed on different days). When F ratios exceeded the critical value ($p \leq 0.05$), the Newman-Keuls test was used for multiple comparisons among experimental means. No differences in P2X2 or P2X3 receptor expression in the spinal cord were observed between male or female postnatal rats with immunostaining. Thus, densitometry data from the DH of male and female postnatal rats were pooled. Descriptions of P2X2 and P2X3 receptor distribution in the spinal cord apply to both male and female postnatal rats.

Western blot, Urinary Bladder

The intensity of each band corresponding to P2X2 or P2X3 was analyzed by semiquantitative image analysis using Un-Scan It software (Silk Scientific, Orem, UT). Background intensities were subtracted from bands of interest. The ratio of the P2X2 or P2X3 protein and corresponding erk1 protein expression is expressed in relative densitometry units. To test for the effect of age on P2X2 or P2X3 expression, linear regression analysis was performed. No differences in P2X2 or P2X3 receptor expression in urinary bladder were observed between male or female postnatal rats with western blotting. Thus, densitometry data from male and female postnatal rats were pooled.

Results

Urinary Bladder Weight

The average weight of the urinary bladder at the earliest postnatal time-point examined (P0) was 15.9 ± 2.5 mg and was significantly ($p \leq 0.001$) less than that determined from P7 through adulthood. As expected, the bladder weight was positively correlated with increasing postnatal age ($R^2 = 0.86$, $p \leq 0.001$). In adult rats, the urinary bladder weight increased to 112.4 ± 5.6 mg.

P2X2 Receptor Expression in Whole Urinary Bladder from Postnatal and Adult Rats

P2X2 receptor expression in whole urinary bladder was greatest ($p \leq 0.005$) at P0-P7 and then exhibited an age dependent decrease in expression ($R^2 = 0.96$) (Fig. 1A, C). P2X2 receptor expression in adult bladder was significantly less than that observed during the first postnatal week (P0-P7). On western blot, the band at 90 kD was blocked by preabsorption of antibody with immunogen (Fig. 1B).

P2X3 Receptor Expression in Whole Urinary Bladder from Postnatal and Adult Rats

P2X3 receptor expression in whole urinary bladder was greatest ($p \leq 0.005$) at P14 compared to expression during the first (P0-P7), fourth (P28), and sixth (P36) postnatal weeks as well as to adult expression (Fig. 2A, C). P2X3 receptor expression was still significantly ($p \leq 0.01$) greater at P21 compared to P0-P7. After P21, P2X3 receptor expression decreased to levels not different from that observed during P0-P7. On western blot, the band at 75 kD was blocked by preabsorption of antibody with immunogen (Fig. 2B).

P2X2 Receptor Expression in Urothelium and Detrusor Smooth Muscle Whole-Mounts from Postnatal and Adult Rats

P2X2-immunoreactivity (IR) was widely distributed in urothelium and detrusor smooth muscle in all postnatal and adult rats (Fig. 3, 4). At birth (P0), P2X2-IR was most prominent in urothelial cells and in the serosal layer of the detrusor smooth muscle (Fig. 3A, D). P2X2-IR was weakly expressed in the suburothelial plexus at birth in bladder trigone or neck (Fig. 3B) and staining in detrusor smooth muscle was also observed (Fig. 3C, G). The intensity of P2X2-IR persisted in the urothelial cells until P14 (Fig. 3E) after which time P2X2-IR decreased (Fig. 4A, E). In contrast, P2X2-IR increased in the suburothelial plexus in bladder trigone and neck with increasing postnatal age (P0-P28; Fig. 3B, F; Fig. 4B) but then decreased at P36 and in adult rats (Fig. 4F). P2X2-IR in nerve fibers associated with detrusor smooth muscle or in detrusor smooth muscle was consistent across all ages (Fig. 3C,G; Fig. 4C,G) and an occasional P2X2-immunoreactive cell was observed adjacent to or embedded in the detrusor smooth muscle both in younger (P14; Fig. 3G, arrow) and adult rats (Fig. 4G, arrow). P2X2-IR in the serosa was consistent among all postnatal ages and adult rats (Fig. 3D, H; Fig. 4D, H). P2X2-immunoreactive fibers in the serosa and suburothelial plexus were immunoreactive for PGP9.5 (Fig. 5A-F). In summary, P2X2-IR remained relatively constant in detrusor smooth muscle with increasing age but decreased in the urothelial cells. P2X2 receptor expression in the subepithelial plexus increased up to P21-P28 then decreased in older neonate and adult rats.

P2X3 Receptor Expression in Urothelium and Detrusor Smooth Muscle Whole-Mounts from Postnatal and Adult Rats

P2X3-immunoreactivity (IR) was initially more restricted in the urinary bladder being present in detrusor smooth muscle and serosa (Fig. 6C, D, G, H) with only weak staining being observed in the urothelial cells and suburothelial plexus in bladder trigone and neck at P2 (Fig. 6B). With increasing postnatal age, P2X3-IR increased in the urothelial cells and in the suburothelial plexus in bladder trigone and neck (Fig. 7A, B, E, F). P2X3-immunoreactive nerve fibers associated with detrusor smooth muscle or in detrusor smooth muscle remained constant at all ages examined. On occasion, individual or small groups of P2X3-immunoreactive cells (Fig. 6C arrows) were observed adjacent to or within detrusor smooth muscle. P2X3-IR was relatively constant in the serosa from P2-adult (Fig. 6D, H; Fig. 7D, H). P2X3-immunoreactive fibers in the serosa and suburothelial plexus were immunoreactive for PGP9.5 (Fig. 5G-L). In summary, P2X3-IR remained relatively constant in detrusor smooth muscle and serosa with increasing postnatal age but P2X3-IR increased in urothelial cells and in suburothelial plexus in bladder trigone and neck with age.

P2X2 Receptor Expression in Postnatal and Adult Lumbosacral Spinal Cord

P2X2-IR in spinal cord was observed by P2 and persisted into adult rat spinal cord (Fig. 8). The distribution of P2X2-IR was distributed in cells lining the central canal (Fig. 8B, D, F) in lumbosacral spinal cord. Although our focus is on the lumbosacral spinal cord, other spinal cord levels (thoracic) were also examined and P2X2-IR was also expressed in this level in some cells lining the central canal. Some of these P2X2-immunoreactive cells had long processes that projected long distances from the central canal (Fig. 8D, F). P2X2-IR was also observed in the epithelial lining of the anterior spinal artery (Fig. 8A, C, E white arrow) and in the anterior corticospinal tract (Fig. 8C, E yellow arrow). Based upon location, we hypothesized that the P2X2-immunoreactive cells lining the central canal were ependyme cells, a specialized type of glial cell. Double-labeling with P2X2- and the pan neuronal marker HuC/D did not reveal any P2X2-immunoreactive cells that also exhibited HuC/D-IR (Fig. 9A-D). P2X2-immunoreactive cells were also not labeled with GFAP and were therefore not astrocytes (Fig. 9E-H). Some studies have indicated that some populations of ependyme cells express immunoreactivity to S-100 protein (17). Although double-labeling for P2X2- and S-100-IR was not possible due to common hosts, single labeling with S-100 did reveal some ependyme cells with a similar morphology to those exhibiting P2X2-IR (Fig. 9H, I white arrows).

P2X3 Receptor Expression in Postnatal and Adult Lumbosacral Spinal Cord Distribution and General Characteristics

In the lumbosacral spinal cord, P2X3-IR was expressed in the superficial dorsal horn (DH) (medial and lateral extent of laminae II) at all postnatal ages and in adult rats (Fig. 10, 11). P2X3-IR in lamina II has been previously described (2,54). In younger postnatal rat pups (P0-P14), P2X3-IR was also present in deeper laminae of the DH (Fig. 10A, C). The labeling in the deeper laminae did not persist in older rat pups or adult rats where the P2X3-IR in the DH was refined and restricted to lamina II (Fig. 11). The percentage of the DH occupied with P2X3-IR nerve fibers increased from that observed at P0 and reached a peak at P21 (Fig. 12A , B). The percentage of the DH occupied with P2X3-immunoreactive nerve fibers from P7-P28 was significantly ($p \leq 0.001$) greater than that at P36 or in adults (Fig. 12B). Intense P2X3-IR was observed in the region of the dorsal commissure (DCM) located dorsal to the central canal (Fig. 10A, C) in younger postnatal rats (P0-14). In the youngest animals examined (P0-P2), P2X3-IR in the DCM was also present in fiber bundles that extended from the DCM ventrally toward the central canal (Fig. 10A,C). These P2X3-immunoreactive fiber bundles were present bilaterally in the L6-S1 spinal segments. After this age, P2X3-IR in the DCM region was noticeably less or absent (Fig. 10E; Fig. 11A, C, E). P2X3-IR was expressed in nerve fibers in specific regions of the spinal cord and had a punctate staining quality. In the spinal cord of rats older than P2, P2X3-IR was not expressed by any cell bodies.

P2X3-IR in the Lateral Collateral Pathway in the L6-S1 Spinal Cord

P2X3-immunoreactive fiber staining in the L6-S1 spinal cord of younger postnatal (P0-P14) rats examined was apparent in a fiber bundle extending ventrally from Lissauer's tract in lamina I along the lateral edge of the dorsal horn into the dorsal part of the sacral parasympathetic nucleus (SPN)(Fig. 10B,D, F) identified by immunostaining for nNOS-IR (51)(Fig. 10B, D, F). The P2X3-IR in LCP of older postnatal and adult rats was less frequently observed and when present, the P2X3-IR was less intense (Fig. 11B, F). The general location of the P2X3-immunoreactive bundle in lamina I and its selective segmental distribution resembles the central projections of visceral afferents in the pelvic nerve which have been labeled in the rat and cat by axonal transport of horseradish peroxidase and designated the lateral collateral pathway of Lissauer's tract (LCP) (33, 42).

Discussion

These studies demonstrate several novel observations related to the plastic expression of P2X2 and P2X3 receptor expression in urinary bladder and spinal cord at times coincident with postnatal maturation of voiding reflexes. Western blot demonstrated an age-dependent decrease in P2X2 receptor expression in bladder whereas P2X3 receptor expression in bladder peaked from P14-P21. P2X2-immunoreactivity (IR) was present in urothelial cells, suburothelial plexus in bladder neck and trigone, detrusor smooth muscle and serosa at birth with staining in urothelial cells and serosa being most predominant. With increasing postnatal age, the intensity of P2X2-IR decreased in urothelial cells but increased in suburothelial plexus. P2X3-IR increased in urothelial cells and suburothelial plexus in bladder neck and trigone with postnatal age whereas staining in detrusor and serosa remained relatively constant. At birth, P2X3-IR was present in the dorsal horn (DH), lateral collateral pathway (LCP) of Lissauer, and dorsal commissure. With increasing age, P2X3-IR was restricted to superficial DH and LCP. P2X2-IR was present in ependyme cells (S-100-IR) of the central canal as early as P2.

Substantial evidence supports a functional role for adenosine triphosphate (ATP) in the modalities of mechanotransduction and nociception in the urinary bladder (7,10,57). ATP may contribute to excitatory neurotransmission in the urinary bladder by acting at P2X receptors in detrusor smooth muscle (38), urothelium (45–47) and afferent nerves in the suburothelial plexus (10). We now demonstrate that P2X receptor expression changes in rat urinary bladder and spinal cord with postnatal development. These changes in P2X2 and P2X3 receptor expression in urinary bladder and spinal cord occur during the second to third postnatal week of birth when a primitive voiding reflex (perigenital-to-bladder reflex) is being replaced by a mature voiding reflex (spinobulbospinal reflex) (12,13).

The non-neuronal location of P2X receptors has been previously demonstrated (5,45,46) and this urothelial distribution has been suggested to play roles in maintenance of barrier function, sensory transduction mechanisms or antigen presentation in host-defense mechanisms (5). The present study extends these findings and demonstrates changes in P2X2 and P2X3 receptor expression primarily in the urothelial cells and suburothelial plexus during rat postnatal development whereas receptor expression in the detrusor smooth muscle and serosa remained relatively constant. Western blot revealed an age dependent decrease in P2X2-IR in the whole urinary bladder. Immunohistochemistry demonstrated that this decrease in P2X2-IR is largely associated with decreased P2X2 receptor expression in the urothelial cells and suburothelial plexus. Previous studies have demonstrated P2X2 receptor expression in detrusor smooth muscle (38) and urothelial cells (47) in humans, rats (30) and cats (5) and this expression is altered in female idiopathic detrusor instability (38), IC (47) and feline IC (5). Previous studies have demonstrated P2X3 receptor expression in human urothelial cells and the suggestion of P2X2/3 heteromers in the urothelium has been made (47).

P2X3 receptor expression in urothelium of adult rat (20) has been demonstrated; however, other studies do not comment on P2X3 staining in the urothelium of rodents (10,30,53). In contrast, P2X3 receptor expression in human and cat urothelium has been demonstrated in cultured urothelial cells (5,44,45,47). In the present study, P2X3 expression in whole rat urinary bladder significantly increased at P14-P21 and then decreased in older rat pups and adults to expression levels not significantly different from that observed from P0-P7. This may suggest that changes in P2X3-IR are driven by changes in the urothelial cells and suburothelial plexus. Expression of the P2X3 receptor in DRG also changes during embryonic and early postnatal mouse development with all DRG cells expressing P2X3 receptor at E14-E16 but only 44.3% of adult mouse DRG cells express P2X3 receptor (40). Our observation of peak P2X2 and P2X3 receptor expression in whole urinary bladder at P14-P21 is consistent with

pharmacologic studies that demonstrate the highest potency of nucleotides on bladder contractile responses between P10 and P25 (8,25,32,36).

Urothelial cells share a number of similarities with sensory neurons and the urothelium has been suggested by Birder et al. (4) to have 'neuronal-like' properties. Urothelial cells express a number of receptors and ion channels similar to those found in sensory neurons (4,28) (34). In the present study, we demonstrate P2X2 and P2X3 receptor expression in urothelium of postnatal and adult rats with reciprocal expression patterns. That is, P2X2 receptor expression in urothelium is greatest in younger postnatal rats and weakest in adult rats whereas the opposite is observed for P2X3 receptor expression. In addition to changes in urothelial cell staining with postnatal development, the suburothelial plexus in the bladder trigone and neck regions also changed expression. P2X3-IR in the suburothelial plexus in the bladder trigone and neck regions increased with postnatal age whereas P2X2-IR in the suburothelial plexus reached a maximum at the fourth postnatal week after which the expression decreased in older postnatal and adult rats. The afferent nerves from humans and other animals have been identified suburothelially (24,55) as well as being scattered throughout the detrusor smooth muscle. Some of these suburothelial nerve fibers exhibit immunoreactivity to calcitonin gene-related peptide (CGRP) (24) and substance P (SP) (55). In addition, some suburothelial nerve fibers exhibit vesicular acetylcholine transporter (VAChT) (18), an indirect indicator of cholinergic nerves. In contrast, abundant VAChT-IR nerve fibers are present in the muscular coat of the urinary bladder (18). The P2X2 and P2X3 receptor staining in the suburothelial plexus and serosal surface of the bladder in this study are suggestive of purinergic receptor distribution in both afferent and efferent nerve fibers.

Changes in P2X3 receptor expression were also observed in the lumbosacral spinal cord during postnatal development whereas P2X2 receptor expression was constant and restricted to ependyme cells surrounding the central canal. P2X3 receptor staining is more intense and more frequently observed in the central afferent projections of visceral afferents (i.e., LCP) in early postnatal development (P0-P14) and P2X3 receptor staining in dorsal horn (DH) peaks at P14-P21. The timing (P14-P21) of the peak increase in P2X3 receptor staining in the DH is similar to the timing of the peak increase in the P2X3-IR in whole urinary bladder at P14-P21. This may suggest that central and peripheral bladder afferents show a similar, developmentally regulated expression of P2X3 receptor. The weak P2X3 receptor staining in the LCP in older postnatal and adult rats is consistent with studies that demonstrate weak P2X3 receptor staining in bladder afferent cells in the DRG (57). In this study, a significant increase in the DH area exhibiting P2X3-IR occurred at P14-P21 compared to P0. This change in receptor expression in the lumbosacral spinal cord in addition to the more widespread distribution of P2X3 receptor expression in deeper laminae of the spinal cord from P0-P14 may contribute to exaggerated spinal reflexes with lower thresholds and greater responses in young animals compared to older animals (22,23). The robust P2X3-IR in the dorsal commissure (DCM) of the lumbosacral spinal cord may also be associated with enhanced visceral responses during the early postnatal period because cells in the DCM are the origin of a visceral pain pathway that ascends in the dorsal columns of the spinal cord (56). In addition, previous studies have revealed increased Fos protein expression in the DCM region after noxious irritation of the urinary bladder (3) or after non-noxious stimulation of the urinary bladder in rats with a cyclophosphamide-induced cystitis (50). Thus, nerve fibers expressing P2X3-IR in the DCM may influence cells in this same region.

The mechanism(s) underlying the changes in P2X2 and P2X3 receptor expression in the postnatal rat bladder and spinal cord in the present study and the development of mature voiding reflexes are not known. Previous studies have suggested that maturation of peptidergic afferent pathways in the urinary bladder of the neonatal rat may be involved in development of mature voiding reflexes (31). However, it has also been demonstrated that regional noradrenergic and

cholinergic neurochemistry of the rat urinary bladder is relatively stable as the rat matures (27). Thus, maturation of peptidergic afferent pathways may play a greater role in the maturation of micturition reflexes compared to adrenergic and cholinergic systems. Maturation of central pathways is also likely to be a factor in the postnatal development of bladder reflexes (6). Neurotrophic factors expressed in the developing urinary bladder may also play a role in synaptic reorganization associated with maturation of micturition reflexes (52). Previous studies (39) have demonstrated that intrathecal administration of NGF or GDNF can either induce or increase expression, respectively, of P2X3 receptor in adult rat spinal cord and DRG.

In summary, these studies demonstrate plasticity in expression of P2X2 and P2X3 receptor subtypes in urinary bladder and spinal cord during early postnatal development in the rat. P2X2 receptor expression demonstrates an age-dependent decrease in bladder that is primarily associated with decreased expression in urothelial cells and suburothelial plexus. In contrast, P2X3 receptor expression increased in bladder from P14-P21 and this increase is primarily associated with changes in urothelial cells and suburothelial plexus. P2X3 receptor expression in DH of the lumbosacral spinal cord also increases from P14-P21 whereas P2X2 receptor expression is relatively constant in the spinal cord. It remains to be determined if changes in P2X receptor expression in bladder or spinal cord play a role in the postnatal maturation of voiding reflexes.

Acknowledgements

A. Torabi was supported, in part, by a Neuroscience Summer Undergraduate Research Fellowship from the University of Vermont, Department of Anatomy and Neurobiology and Neurology. The authors thank Ms. Vivian Hu for technical assistance.

References

1. Andersson KE, Wein AJ. Pharmacology of the lower urinary tract: basis for current and future treatments of urinary incontinence. Pharmacol Rev 2004;56:581–631. [PubMed: 15602011]
2. Barclay J, Patel S, Dorn G, Wotherspoon G, Moffatt S, Eunson L, Abdel'al S, Natt F, Hall J, Winter J, Bevan S, Wishart W, Fox A, Ganju P. Functional downregulation of P2X3 receptor subunit in rat sensory neurons reveals a significant role in chronic neuropathic and inflammatory pain. J Neurosci 2002;22:8139–8147. [PubMed: 12223568]
3. Birder LA, de Groat WC. Induction of c-fos gene expression in spinal neurons of the rat by nociceptive and non-nociceptive stimulation of the lower urinary tract. Am J Physiol 1993;265:R643–R648.
4. Birder LA, Kanai AJ, deGroat WC, Kiss S, Nealen ML, Burke NE, Dineley KE, Watkins S, Reynolds IJ, Caterina MJ. Vanilloid receptor expression suggests a sensory role for urinary bladder epithelial cells. Proc Natl Acad Sci USA 2001;98:13396–13401. [PubMed: 11606761]
5. Birder LA, Ruan HZ, Chopra B, Xiang Z, Barrick S, Buffington CA, Roppolo JR, Ford AP, de Groat WC, Burnstock G. Alterations in P2X and P2Y purinergic receptor expression in urinary bladder from normal cats and cats with interstitial cystitis. Am J Physiol 2004;287:F1084–1091.
6. Bregman BS. Development of serotonin immunoreactivity in the rat spinal cord and its plasticity after neonatal spinal cord lesions. Dev Brain Res 1987;34:245–263.
7. Burnstock G. Purine-mediated signalling in pain and visceral perception. Trends Pharm Sci 2001;22:182–188. [PubMed: 11282418]
8. **Burnstock G** Purinergic signalling in lower urinary tract. In: *Purinergic and Pyrimidinergic Signalling I*, edited by Abbracchio MP and Williams M. New York: Springer-Verlag, 2001, p. 423–515.
9. Capek K, Jelinek J. The development of the control of water metabolism. I. The excretion of urine in young rats. Physiol Bohemoslov 1956;5:91–96. [PubMed: 13349444]
10. Cockayne DA, Hamilton SG, Zhu QM, Dunn PM, Zhong Y, Novakovic S, Malmberg AB, Cain G, Berson A, Kassotakis L, Hedley L, Lachnit WG, Burnstock G, McMahon SB, Ford APDW. Urinary bladder hyporeflexia and reduced pain-related behaviour in P2X(3)-deficient mice. Nature 2000;407:1011–1015. [PubMed: 11069181]

11. de Groat WC. Nervous control of the urinary bladder of the cat. Brain Res 1975;87:201–211. [PubMed: 1125771]
12. de Groat WC, Araki I. Maturation of bladder reflex pathways during postnatal development. Adv Exp Med Biol 1999;462:253–263. [PubMed: 10599429]discussion 311–220
13. de Groat WC, Araki I, Vizzard MA, Yoshiyama M, Yoshimura N, Sugaya K, Tai C, Roppolo JR. Developmental and injury induced plasticity in the micturition reflex pathway. Behav Brain Res 1998;92:127–140. [PubMed: 9638955]
14. **de Groat WC, Booth AM, and Yoshimura N** Neurophysiology of micturition and its modification in animal models of human disease. In: *The Autonomic Nervous System*, edited by Maggi CA. London: Harwood Academic Publishers, 1993, p. 227–290.
15. **de Groat WC and Kruse MN** Central processing and morphological plasticity in lumbosacral afferent pathways from the lower urinary tract. In: *Basic and Clinical Aspects of Chronic Abdominal Pain. Pain Research and Clinical Management*, edited by Mayer EA and Raybould HE. Amsterdam: Elsevier Science Publishers, 1993, p. 219–235.
16. de Groat WC, Nadelhaft I, Milne RJ, Booth AM, Morgan C, Thor K. Organization of the sacral parasympathetic reflex pathways to the urinary bladder and large intestine. J Auton Nerv Syst 1981;3:135–160. [PubMed: 6268684]
17. Didier M, Harandi M, Aguera M, Bancel B, Tardy M, Fages C, Calas A, Stagaard M, Mollgard K, Belin MF. Differential immunocytochemical staining for glial fibrillary acidic (GFA) protein, S-100 protein and glutamine synthetase in the rat subcommissural organ, nonspecialized ventricular ependyma and adjacent neuropil. Cell Tissue Res 1986;245:343–351. [PubMed: 2874885]
18. Dixon JS, Jen PY, Gosling JA. The distribution of vesicular acetylcholine transporter in the human male genitourinary organs and its co-localization with neuropeptide Y and nitric oxide synthase. Neurourol Urodyn 2000;19:185–194. [PubMed: 10679835]
19. Ekstrom J, Ekman R, Hakanson R. Ontogeny of neuropeptides in the rat urinary bladder. Regul Pept 1994;50:23–28. [PubMed: 7512739]
20. Elneil S, Skepper JN, Kidd EJ, Williamson JG, Ferguson DR. Distribution of P2X(1) and P2X(3) receptors in the rat and human urinary bladder. Pharmacology 2001;63:120–128. [PubMed: 11490205]
21. Ferguson DR, Kennedy I, Burton TJ. ATP is released from rabbit urinary bladder epithelial cells by hydrostatic pressure changes--a possible sensory mechanism? J Physiol 1997;505 (Pt 2):503–511. [PubMed: 9423189]
22. Fitzgerald M, Beggs S. The neurobiology of pain: developmental aspects. Neuroscientist 2001;7:246–257. [PubMed: 11499403]
23. Fitzgerald M, Jennings E. The postnatal development of spinal sensory processing. Proc Natl Acad Sci USA 1999;96:7719–7722. [PubMed: 10393887]
24. Gabella G, Davis C. Distribution of afferent axons in the bladder of rats. J Neurocytol 1998;27:141–155. [PubMed: 10640174]
25. Hourani SM. Postnatal development of purinoceptors in rat visceral smooth muscle preparations. Gen Pharmacol 1999;32:3–7. [PubMed: 9888246]
26. Iuchi H, Satoh Y, Ono K. Postnatal development of neuropeptide Y-and calcitonin gene-related peptide-immunoreactive nerves in the rat urinary bladder. Anat Embryol (Berl) 1994;189:361–373. [PubMed: 8074324]
27. Johnson JM, Skau KA, Gerald MC, Wallace LJ. Regional noradrenergic and cholinergic neurochemistry in the rat urinary bladder: effect of age. J Urol 1988;139:611–615. [PubMed: 2893842]
28. Keast JR, Kepper ME. Differential regulation of trkA and p75 in noradrenergic pelvic autonomic ganglion cells after deafferentation of their cholinergic neighbours. Eur J Neurosci 2001;13:211–220. [PubMed: 11168525]
29. Kruse MN, de Groat WC. Changes in lower urinary tract function following spinal cord injury. J Restor Neurol Neurosci 1993;5:79–80.
30. Lee HY, Bardini M, Burnstock G. Distribution of P2X receptors in the urinary bladder and the ureter of the rat. J Urol 2000;163:2002–2007. [PubMed: 10799247]

31. Maggi CA, Santicioli P, Geppeti S, Frilli MG, Spillantini MG, Nediani C, Hunt SP, Meli A. Biochemical, anatomical and functional correlates of postnatal developments of the capsaicin-sensitive innervation of the rat urinary bladder. Dev Brain Res 1988;43:183–190.
32. Maggi CA, Santicioli P, Meli A. Postnatal development of myogenic contractile activity and excitatory innervation of rat urinary bladder. Am J Physiol 1984;247:R972–978. [PubMed: 6150648]
33. Morgan C, Nadelhaft I, de Groat WC. The distribution of visceral primary afferents from the pelvic nerve within Lissauer's tract and the spinal gray matter and its relationship to the sacral parasympathetic nucleus. J Comp Neurol 1981;201:415–440. [PubMed: 7276258]
34. Murray E, Malley SE, Qiao LY, Hu VY, Vizzard MA. Cyclophosphamide induced cystitis alters neurotrophin and receptor tyrosine kinase expression in pelvic ganglia and bladder. J Urol 2004;172:2434–2439. [PubMed: 15538286]
35. Nicholls J, Hourani SM, Kitchen I. Degradation of extracellular adenosine and ATP by adult and neonatal rat duodenum and urinary bladder. Pharmacol Comm 1992;2:203–210.
36. Nicholls J, Hourani SM, Kitchen I. The ontogeny of purinoceptors in rat urinary bladder and duodenum. Br J Pharmacol 1990;100:874–878. [PubMed: 2207506]
37. North RA. Molecular physiology of P2X receptors. Physiol Rev 2002;82:1013–1067. [PubMed: 12270951]
38. O'Reilly BA, Kosaka AH, Knight GF, Chang TK, Ford AP, Rymer JM, Popert R, Burnstock G, McMahon SB. P2X receptors and their role in female idiopathic detrusor instability. J Urol 2002;167:157–164. [PubMed: 11743296]
39. Ramer MS, Bradbury EJ, McMahon SB. Nerve growth factor induces P2X(3) expression in sensory neurons. J Neurochem 2001;77:864–875. [PubMed: 11331415]
40. Ruan HZ, Moules E, Burnstock G. Changes in P2X3 purinoceptors in sensory ganglia of the mouse during embryonic and postnatal development. Histochem Cell Biol 2004;122:539–551. [PubMed: 15549366]
41. Sann H, Walb G, Pierau FK. Postnatal development of the autonomic and sensory innervation of the musculature in the rat urinary bladder. Neurosci Lett 1997;236:29–32. [PubMed: 9404944]
42. Steers WD, Ciambotti J, Etzel B, Erdman S, de Groat WC. Alterations in afferent pathways from the urinary bladder of the rat in response to partial urethral obstruction. J Comp Neurol 1991;310:1–10. [PubMed: 1658087]
43. Studeny S, Torabi A, Vizzard MA. P2X2 and P2X3 receptor expression in postnatal rat urinary bladder and lumbosacral spinal cord: a developmental study. Urothelial Cell Physiology in Normal and Disease States 2005;63
44. Sun Y, Chai TC. Up-regulation of P2X3 receptor during stretch of bladder urothelial cells from patients with interstitial cystitis. J Urol 2004;171:448–452. [PubMed: 14665953]
45. Sun Y, Keay S, De Deyne PG, Chai TC. Augmented stretch activated adenosine triphosphate release from bladder uroepithelial cells in patients with interstitial cystitis. J Urol 2001;166:1951–1956. [PubMed: 11586266]
46. Sun Y, MaLossi J, Jacobs SC, Chai TC. Effect of doxazosin on stretch-activated adenosine triphosphate release in bladder urothelial cells from patients with benign prostatic hyperplasia. Urology 2002;60:351–356. [PubMed: 12137852]
47. Tempest HV, Dixon AK, Turner WH, Elneil S, Sellers LA, Ferguson DR. P2X and P2X receptor expression in human bladder urothelium and changes in interstitial cystitis. BJU Int 2004;93:1344–1348. [PubMed: 15180635]
48. Thor KB, Hisamitsu T, de Groat WC. Unmasking of a neonatal somatovesical reflex in adult cats by the serotonin autoreceptor agonist 5-methoxy-N,N-dimethyltryptamine. Dev Brain Res 1990;54:35–42. [PubMed: 2364543]
49. **Thor KB, Kawatani M, and de Groat WC** Plasticity in the reflex pathways to the lower urinary tract of the cat during postnatal development and following spinal injury. In: *Development and Plasticity of the Mammalian Spinal Cord*, edited by Goldberger ME, Gorio A and Murray M. Padova: Liviana, 1986, p. 65–81.
50. Vizzard MA. Increased expression of spinal Fos protein in lower urinary tract pathways induced by bladder distension following chronic cystitis. Am J Physiol 2000;279:R295–R305.

51. Vizzard MA, Erdman SL, de Groat WC. Increased expression of neuronal nitric oxide synthase (NOS) in visceral neurons after nerve injury. J Neurosci 1995;15:4033–4045. [PubMed: 7538569]
52. Vizzard MA, Wu KH, Jewett IT. Developmental expression of urinary bladder neurotrophic factor mRNA and protein in the neonatal rat. Dev Brain Res 2000;119:217–224. [PubMed: 10675771]
53. Vlaskovska M, Kasakov L, Rong W, Bodin P, Bardini M, Cockayne DA, Ford AP, Burnstock G. P2X3 knock-out mice reveal a major sensory role for urothelially released ATP. J Neurosci 2001;21:5670–5677. [PubMed: 11466438]
54. Vulchanova L, Riedl MS, Shuster SJ, Stone LS, Hargreaves KM, Buell G, Surprenant A, North RA, Elde R. P2X3 is expressed by DRG neurons that terminate in inner lamina II. Eur J Neurosci 1998;10:3470–3478. [PubMed: 9824460]
55. Wakabayashi Y, Tomoyoshi T, Fujimiya M, Arai R, Maeda T. Substance P-containing axon terminals in the mucosa of the human urinary bladder: pre-embedding immunohistochemistry using cryostat sections for electron microscopy. Histochemistry 1993;100:401–407. [PubMed: 7512948]
56. Willis WD, AlChaer ED, Quast MJ, Westlund KN. A visceral pain pathway in the dorsal column of the spinal cord. Proc Natl Acad Sci USA 1999;96:7675–7679. [PubMed: 10393879]
57. Zhong Y, Banning AS, Cockayne DA, Ford AP, Burnstock G, McMahon SB. Bladder and cutaneous sensory neurons of the rat express different functional P2X receptors. Neuroscience 2003;120:667–675. [PubMed: 12895508]
58. Zvarova K, Murray E, Vizzard MA. Changes in galanin immunoreactivity in rat lumbosacral spinal cord and dorsal root ganglia after spinal cord injury. J Comp Neurol 2004;475:590–603. [PubMed: 15236239]
59. **Zvarova K and Vizzard MA** Distribution and fate of cocaine- and amphetamine-regulated transcript peptide (CARTp) expressing cells in rat urinary bladder: a developmental study. *J Comp Neurol*, in press.

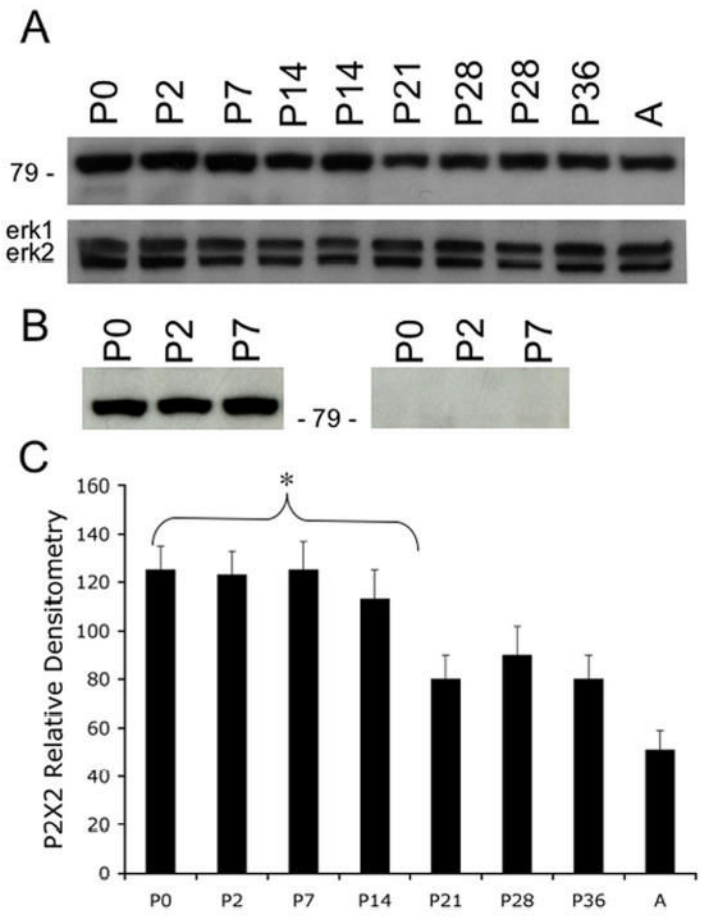

Figure 1.

A. Western blot of whole urinary bladder (40 mg) for P2X2 receptor expression in postnatal (P0-P36) and adult (A) rats. Erk staining was used as a loading control. **B**. Preabsorption of P2X2 antibody with immunogen (1 mg ml^{-1}) eliminated the band at 90kD. **C**. Histogram of relative P2X2 band density in all groups examined normalized to erk-1 staining. P2X2 receptor expression in urinary bladder demonstrated an age-dependent ($R^2 = 0.96$, $p \leq 0.005$) decrease in expression. P2X2 receptor expression in urinary bladder from P0-P14 is significantly greater compared to adult expression. *, $p \leq 0.005$.

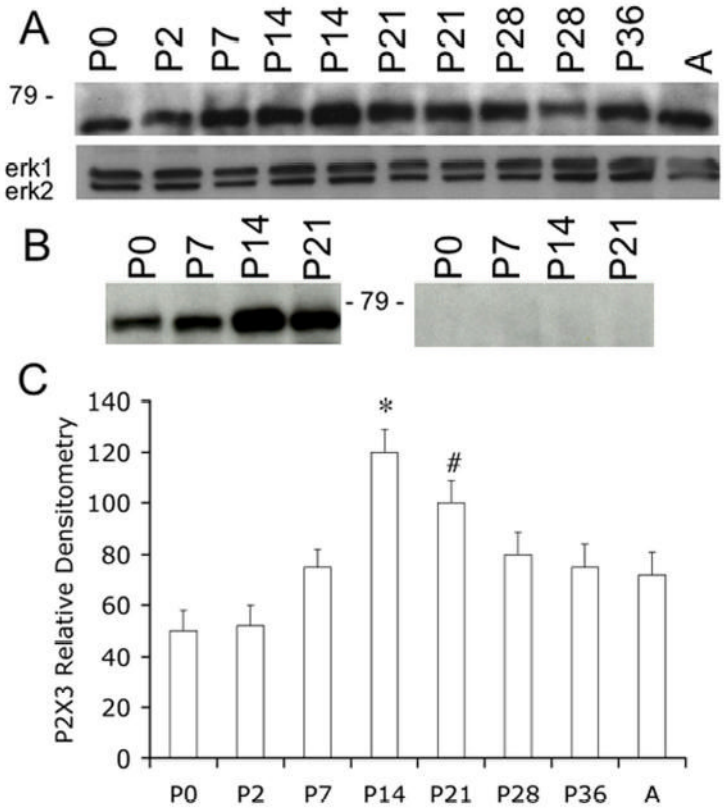

Figure 2.

A. Western blot of whole urinary bladder (40 mg) for P2X3 receptor expression in postnatal (P0-P36) and adult (A) rats. Erk staining was used as a loading control. **B**. Preabsorption of P2X3 antibody with immunogen (1 mg ml^{-1}) eliminated the band at 75kD. **C**. Histogram of relative P2X3 band density in all groups examined normalized to erk-1 staining. P2X3 receptor expression in urinary bladder is significantly increased from P14-P21 compared to adult rat bladder. *, $p \leq 0.005$, #, $p \leq 0.01$.

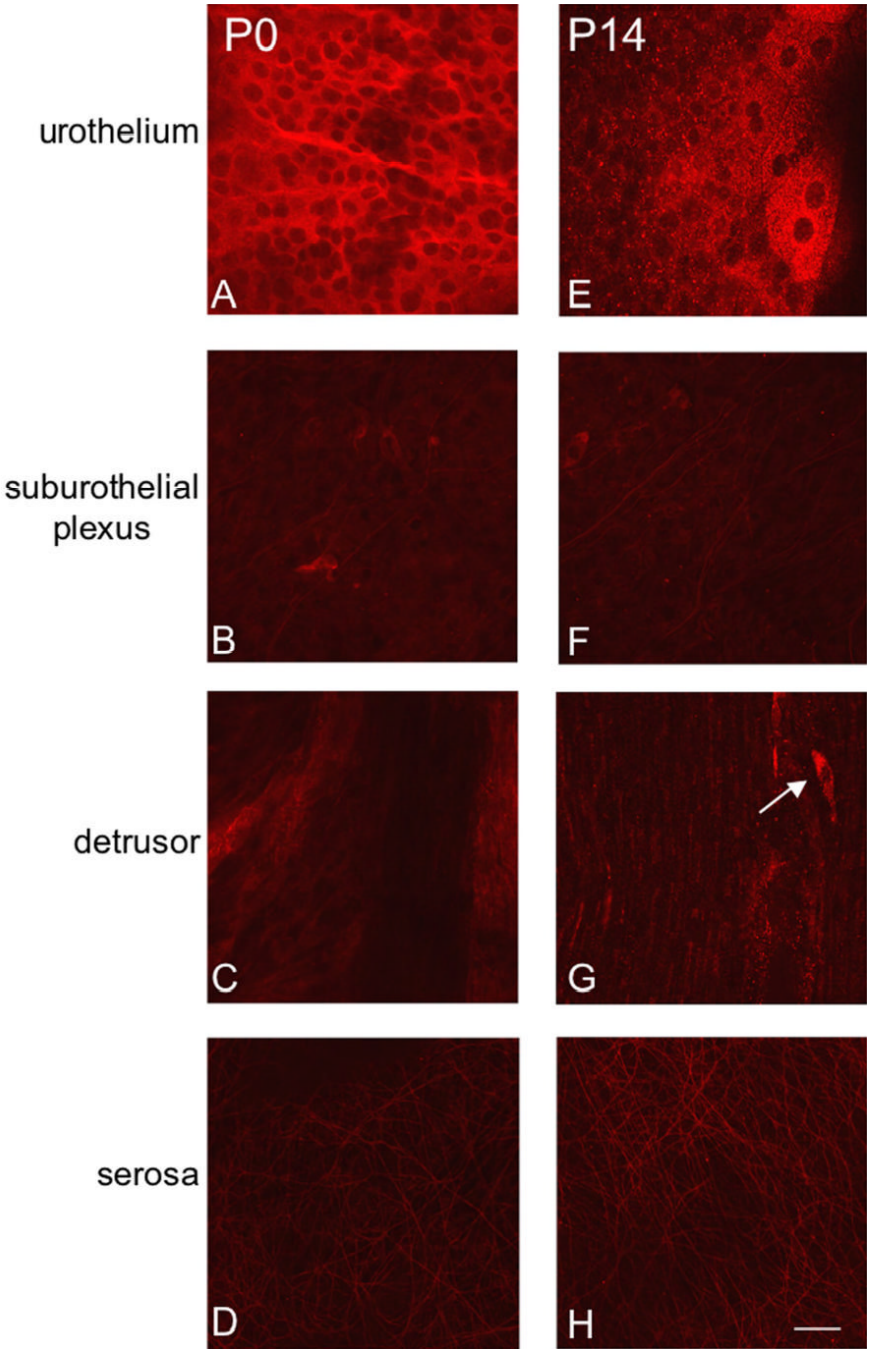

Figure 3.

Fluorescence images of P2X2 receptor expression in urothelium (A, E), suburothelial plexus in bladder neck or trigone (B, F), detrusor (C, G) and serosa (D, H) from postnatal rats, P0-P14. For all images, exposure times were held constant. Expression of P2X2 receptor in the detrusor and serosa was relatively constant. On occasion, P2X2-IR cells were observed in close proximity or adjacent to detrusor smooth muscle (G, arrow). P2X2 receptor expression was intense in urothelial cells but relatively weak in the suburothelial plexus. Calibration bar represents 50 μm.

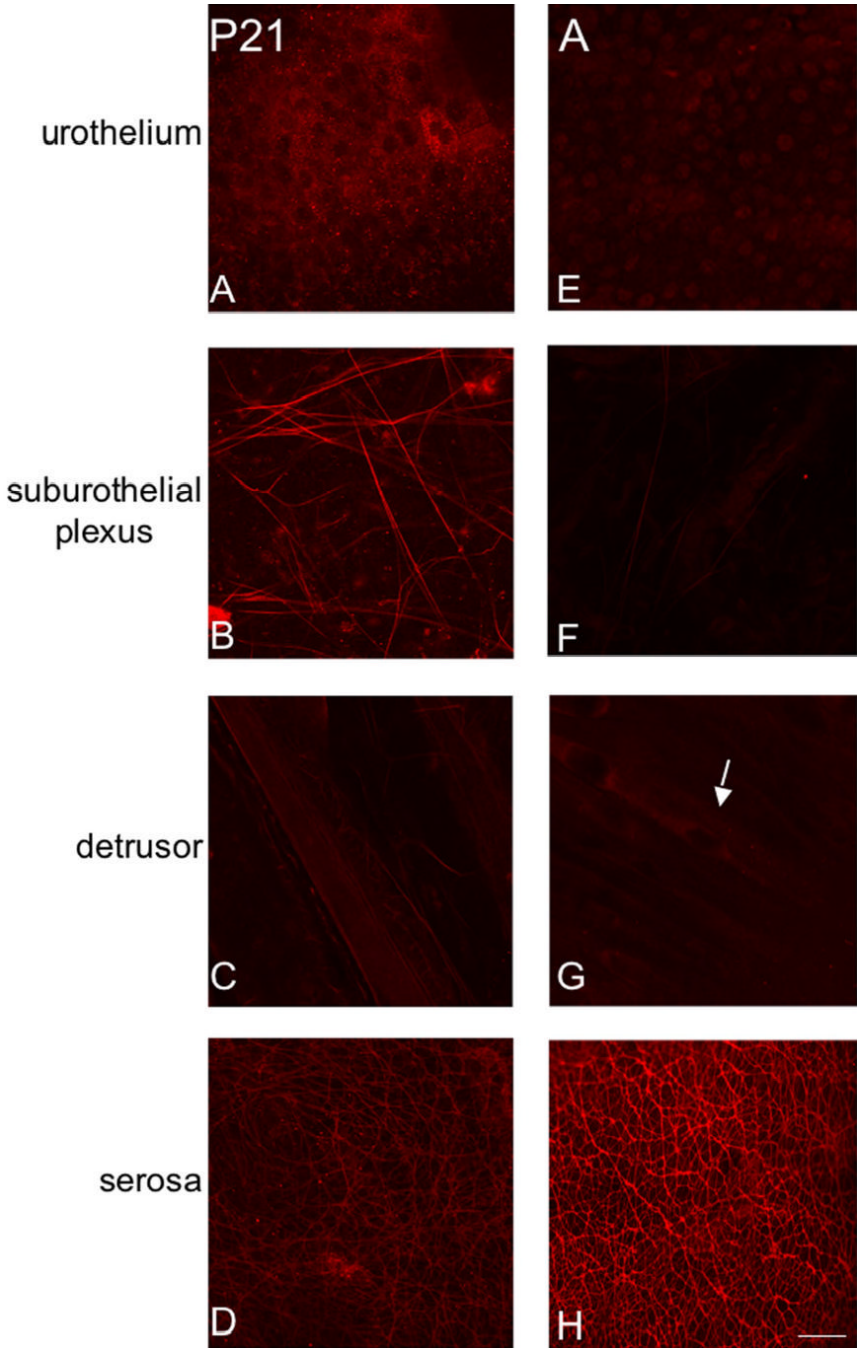

Figure 4.

Fluorescence images of P2X2 receptor expression in urothelium (A, E), suburothelial plexus in bladder neck or trigone (B, F), detrusor (C, G) and serosa (D, H) from postnatal rats, P21-adult (A). For all images, exposure times were held constant. From P21-A, P2X2 receptor expression in detrusor and serosa was relatively constant and P2X2-IR cells were still occasionally observed adjacent to detrusor smooth muscle (G, arrow). P2X2 receptor expression in urothelial cells from P21-A was dramatically reduced compared to that observed from P0-P14. The suburothelial plexus staining for P2X2 receptor in bladder neck or trigone increased from P21-P28 and then staining decreased to that observed from P0-P14. Calibration bar represents 50 μm.

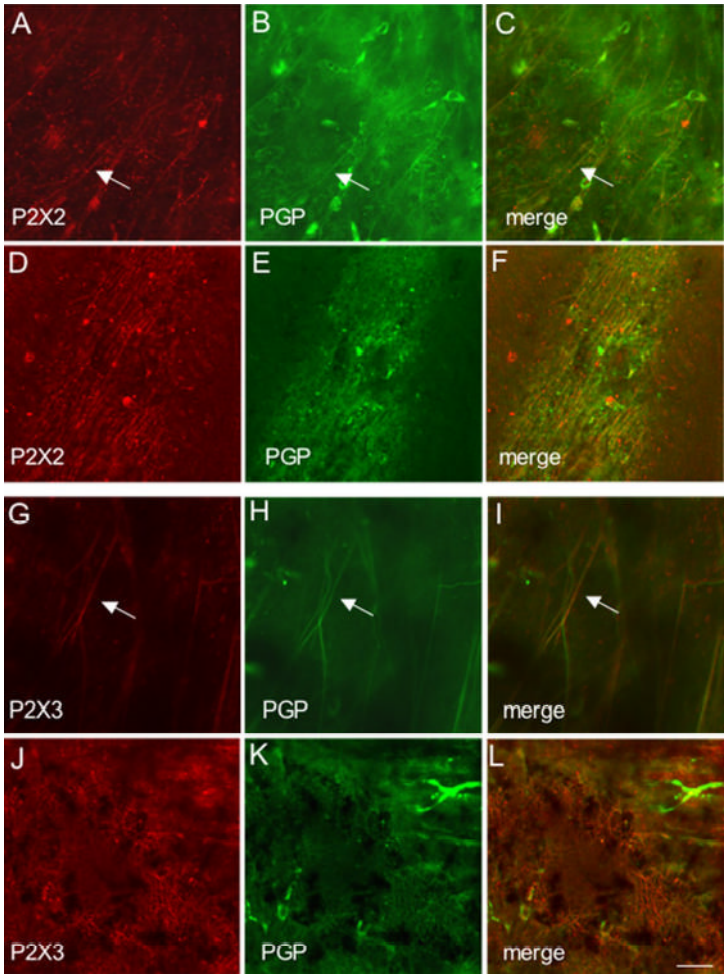

Figure 5.

Fluorescence images of P2X2 (A-F) or P2X3 (G-L) receptor expression in the suburothelial plexus (A-C; G-I) and serosa (D-F; J-L) of adult animals. Whole mounts were also stained for protein gene product (PGP9.5) (B,E,H,K) to confirm that P2X2 and P2X3-immunoreactive structures were nerve fibers. In all tissues examined, the P2X2 and P2X3-IR in the suburothelial plexus or serosa was colabeled with PGP9.5. Merged images (C,F,I,L) demonstrating overlap between P2X2 and PGP9.5 (C,F) or P2X3 and PGP9.5 (I,L). Some isolated nerve fibers demonstrating P2X2- and PGP9.5-IR (C, arrow) or P2X3-and PGP9.5-IR (I, arrow) are shown in the suburothelial plexus. Calibration bar represents 50 μm.

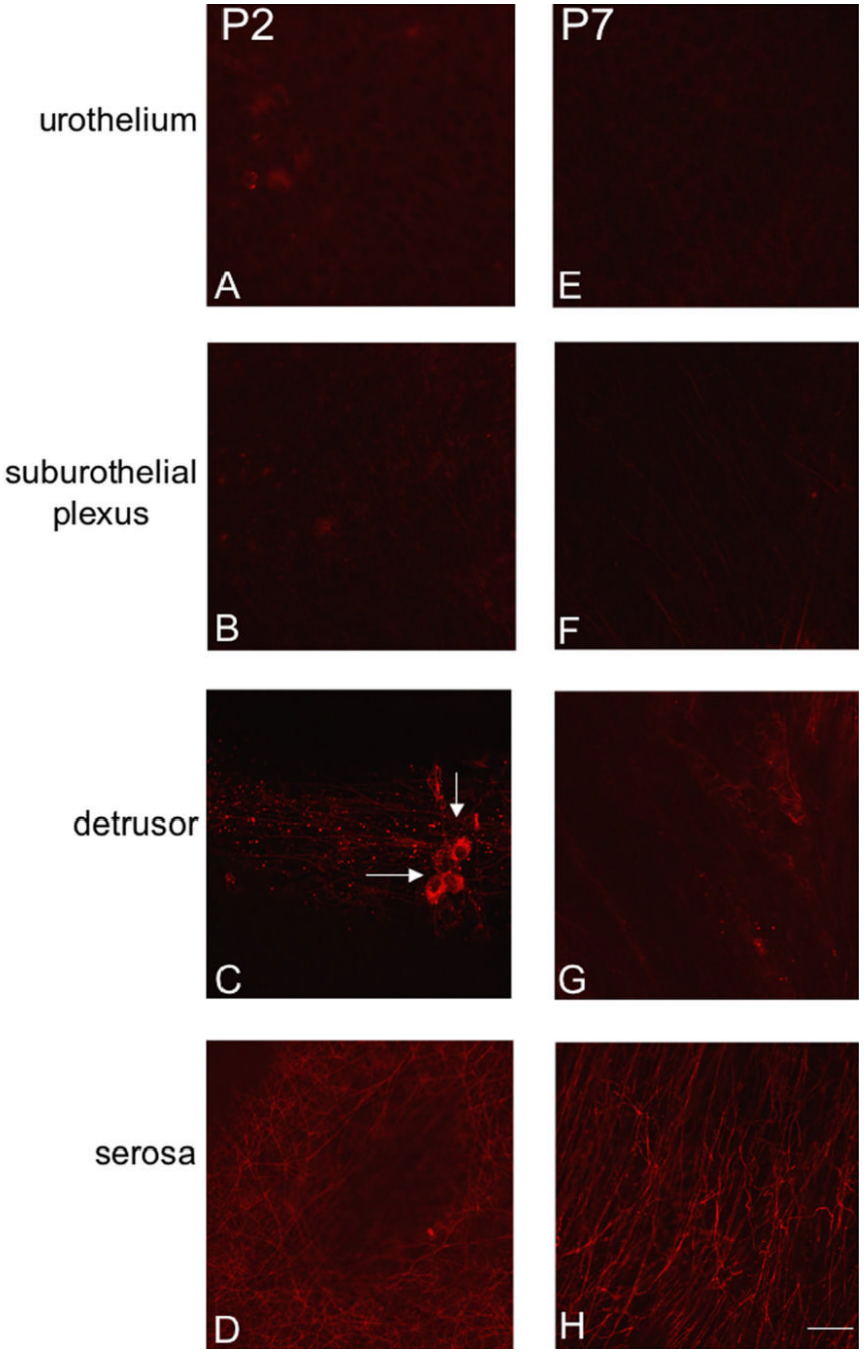

Figure 6.

Fluorescence images of P2X3 receptor expression in urothelium (A, E), suburothelial plexus in bladder trigone or neck (B, F), detrusor (C, G) and serosa (D, H) from postnatal rats, P2-P7. For all images, exposure times were held constant. Expression of P2X3 receptor in the detrusor and serosa was relatively constant. On occasion, isolated or small groups of P2X3-IR cells were observed in close proximity or adjacent to detrusor smooth muscle (C, arrows). P2X3 receptor expression was weak in urothelial cells and sparse P2X3-IR was observed in the suburothelial plexus from P0-P14. Calibration bar represents 50 μm.

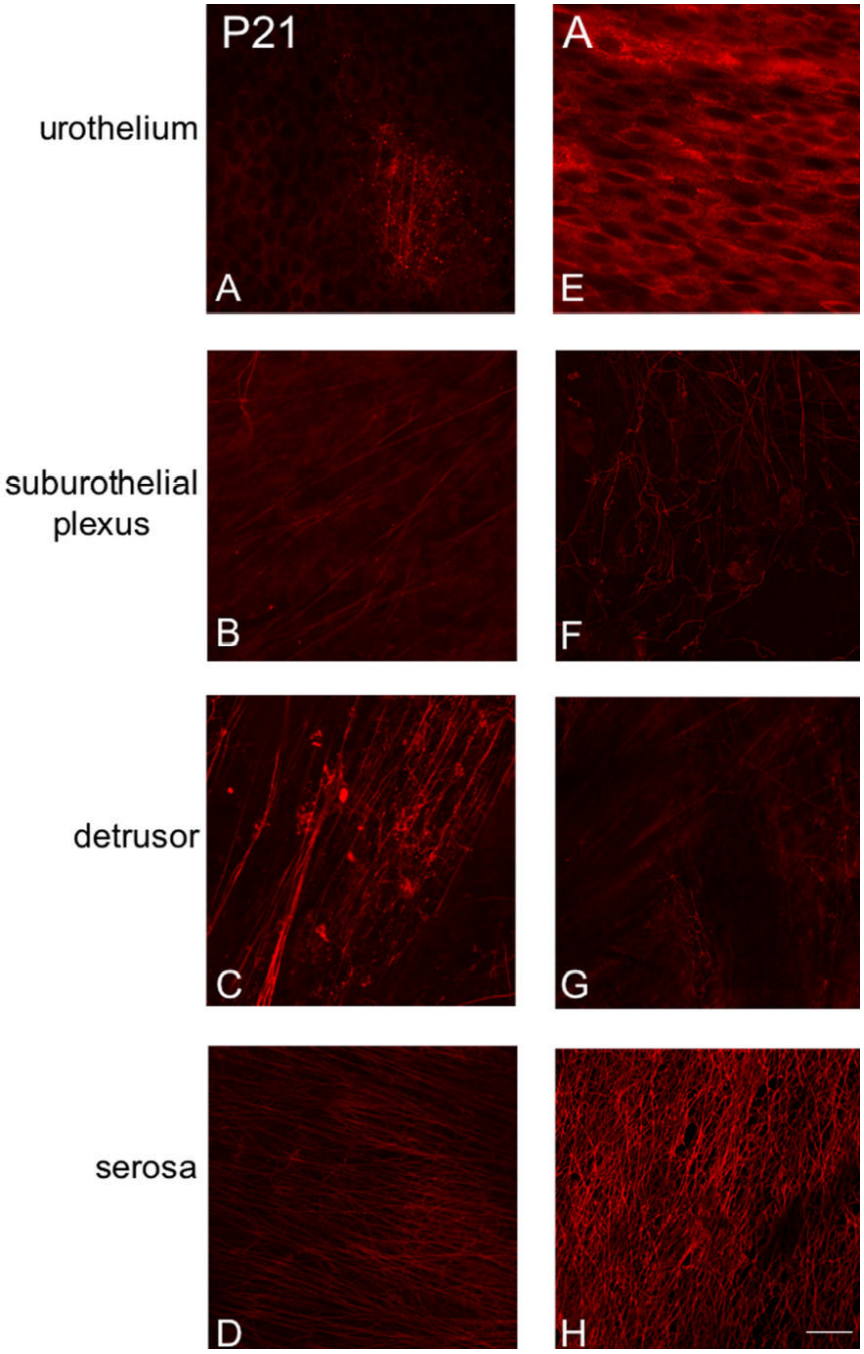

Figure 7.

Fluorescence images of P2X3 receptor expression in urothelium (A, E) suburothelial plexus in bladder trigone or neck (B, F), detrusor (C, G) and serosa (D, H) from postnatal rats, P21-adult (A). For all images, exposure times were held constant. Expression of P2X3 receptor in the detrusor and serosa was relatively constant. P2X3 receptor expression increased in urothelial cells from P21 through adulthood and a more extensive P2X3-IR suburothelial nerve plexus was observed in the bladder trigone and neck from P21 through adult. Calibration bar represents 50 μm.

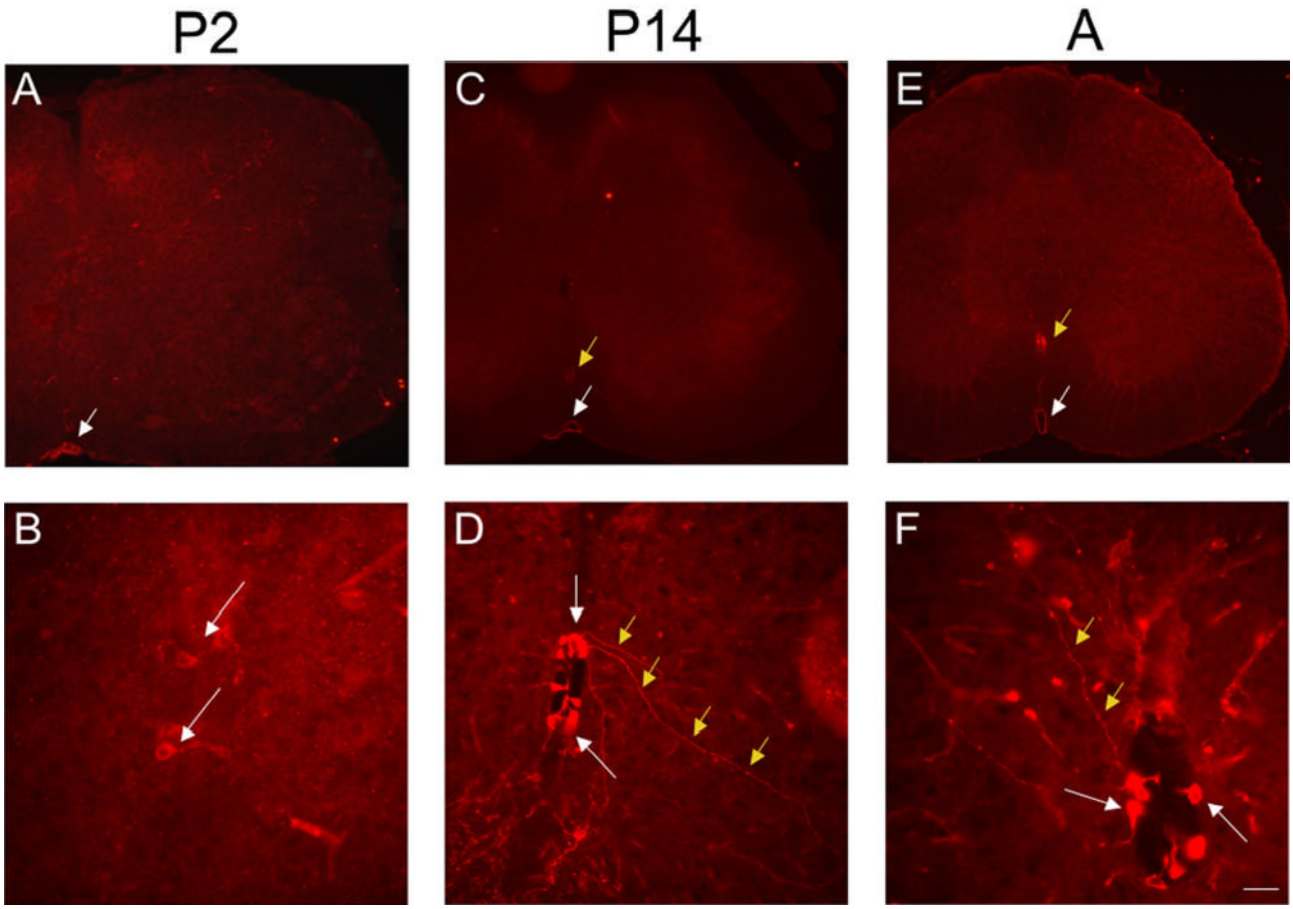

Figure 8.

P2X2 receptor expression in cells lining the central canal (CC) of the lumbosacral spinal cord from P2-adult (A). As early as P2 (A, B), P2X2-IR cells (B, arrows) were observed surrounding the CC but no staining was present at P0. Similar P2X2-immunoreactive cells surrounding the CC were observed at P14 (D, white arrows) and A (F, white arrows). In some instances, long processes could be observed emerging from these P2X2-immunoreactive cells and projecting from the CC laterally and ventrally (D, F, yellow arrows). P2X2-IR was also expressed in the anterior spinal artery (A, C, E, white arrow) and in the anterior corticospinal tract (C, E, yellow arrow). Calibration bar represents 120 μm in A, C, E and 60 μm in B, D.

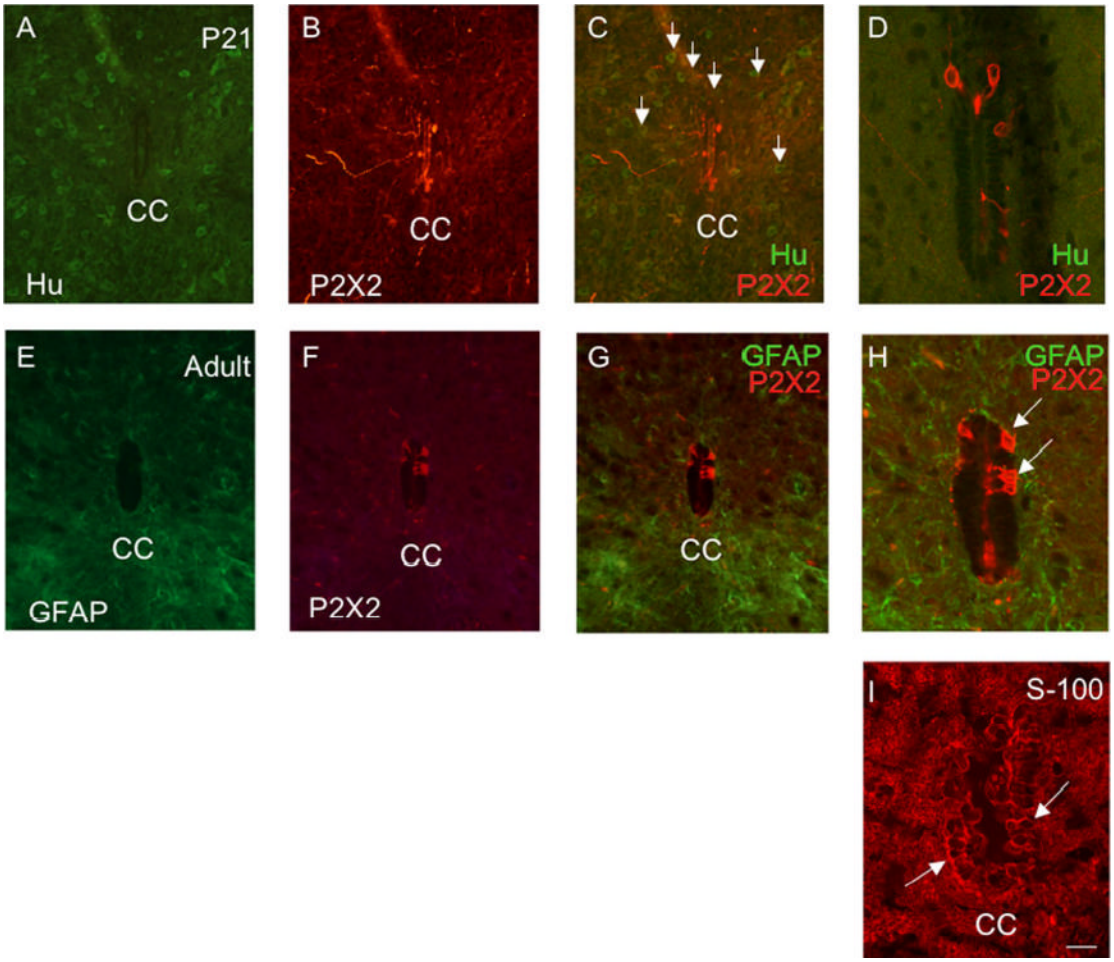

Figure 9.

P2X2-immunoreactive cells lining the central canal (CC) are presumptive ependyme cells, modified glial cells. P2X2-immunoreactive cells lining the CC did not exhibit immunoreactivity to the pan neuronal marker, HuC/D (A-D) and were therefore not neuronal. Numerous HuC/D-immunoreactive cells were present throughout the spinal cord parenchyma (C, arrows) but P2X2-immunoreactive cells did not exhibit HuC/D-IR (C, D). C, D are merged images demonstrating P2X2- (red) and HuC/D-IR (green). In addition, P2X2-IR cells surrounding the CC did not exhibit immunoreactivity to glial fibrillary acidic protein (GFAP) (E, G, H) and were therefore not astrocytes (E-H). G, H are merged images demonstrating P2X2- (red) and GFAP-IR (green) surrounding the CC. Some ependyme cells express immunoreactivity to the protein S-100 (19). S-100-IR cells (I) were observed surrounding the CC and many of these cells expressed a similar morphology to the P2X2-IR cells (D, H versus I) surrounding the CC. Calibration bar represents 60 μm.

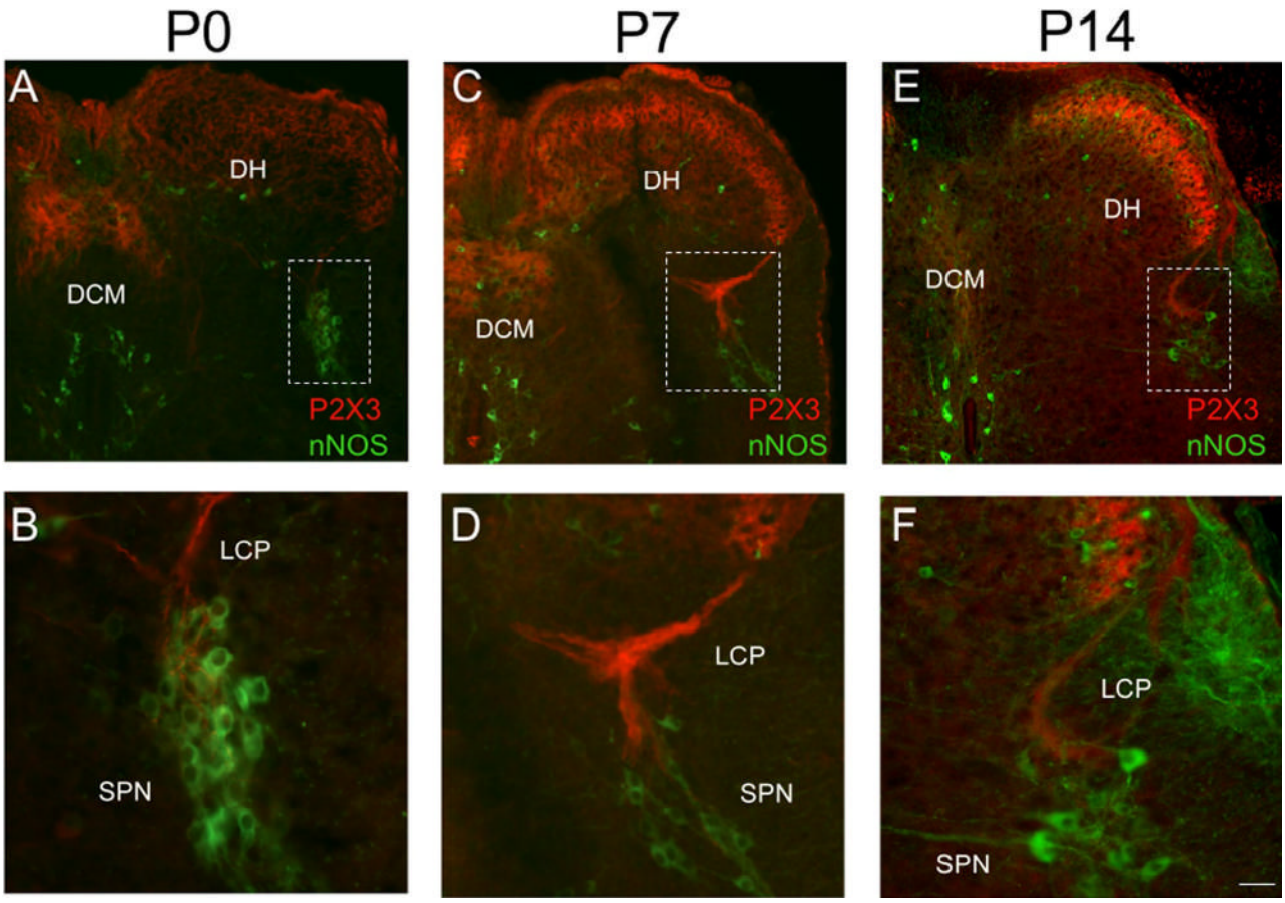

Figure 10.

P2X3-IR in lumbosacral spinal cord from young postnatal (P0-P14) rats. Low power images of P2X3-IR in lumbosacral spinal cord from P0 (A), P7 (C) and P14 (E). To demonstrate the location of the sacral parasympathetic nucleus (SPN) in these young rat pups, tissues were stained for neuronal nitric oxide synthase (nNOS, green; A-F). In animals from P0-P7, P2X3-IR was diffusely distributed in the dorsal horn being present in lamina II but in deeper laminae as well (A, C). In addition, dense P2X3-immunoreactive fiber bundles were present in the dorsal commissure (DCM; A, C). Higher power images (B, D, F) of the boxed regions in A, C, E that demonstrate P2X3-IR (red) in close association with nNOS-IR cells (green). Prominent P2X3-IR (red) was present in the lateral collateral pathway (LCP) of Lissauer extending from lamina I to the region of the SPN (B, D, F). Reduction in P2X3-IR in the DCM and LCP was apparent by P14 (E). By P14, P2X3-IR was more restricted to lamina II in the DH (E). Calibration bar represents 80 μm in A, C, E and 50 μm in B, D, F.

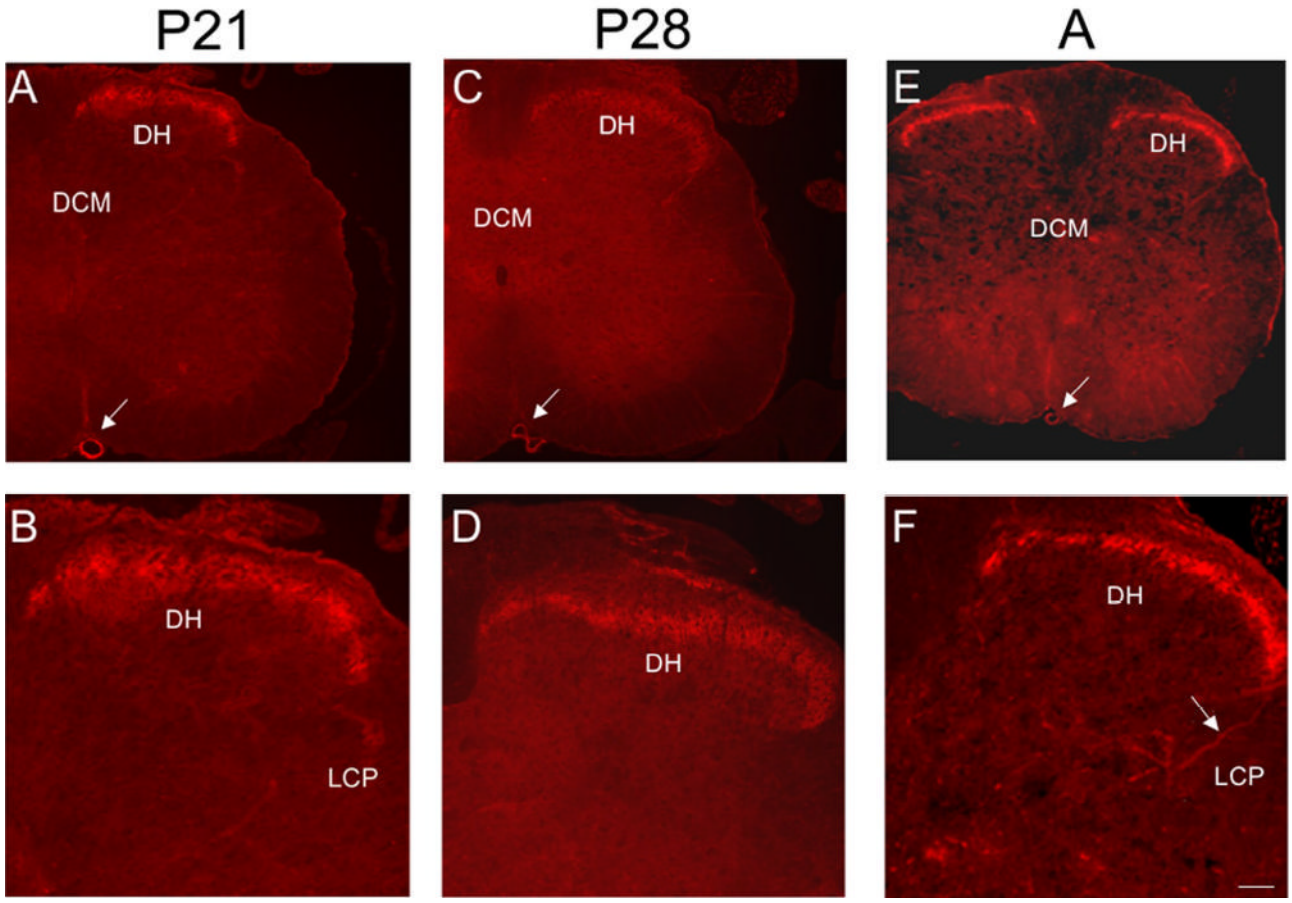

Figure 11.

P2X3-IR in lumbosacral spinal cord from older postnatal (P21-P28) and adult (A) rats. Low power fluorescence images of the L6 spinal cord showing restricted P2X3-IR in the superficial dorsal horn (DH; A, C, E). Higher power fluorescence images of the dorsal, lateral quadrant of the L6 spinal cord showing restricted P2X3-IR in lamina II (B, D, F). Weak P2X3-IR was present in the lateral collateral pathway (LCP) of Lissauer in the lumbosacral spinal cord (F, arrows) of older postnatal and adult rats. P2X3-IR was observed in the anterior spinal artery (A, C, E, arrow). Calibration bar represents 100 μm in A, C, E and 60 μm in B, D, F.

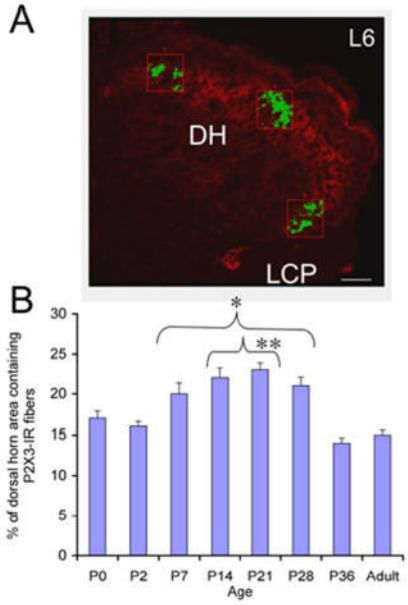

Figure 12.

A. The area occupied by P2X3-immunoreactive nerve fibers in three representative regions of the superficial dorsal horn (DH) in lamina II (lateral, medial and intermediate) of the L6 spinal cord was determined and averaged across spinal cord sections and ages analyzed. Only P2X3-immunoreactive nerve fibers (green) that exceeded the threshold level were quantified. **B**. Summary histogram of the percentage (%) of the DH area containing P2X3-immunoreactive nerve fibers during postnatal (P0-P36) development and adulthood of the rat. The percentage of the DH occupied by P2X3-immunoreactive nerve fibers significantly (*, $p \leq 0.001$) increased from P7-P28 compared to adult. In addition, the percentage of the DH occupied by P2X3-immunoreactive nerve fibers was significantly (#, $p \leq 0.001$) increased from P14-P21 compared to P0. Calibration bar represents 40 μm.

Table 1

Table of primary and secondary antibodies, working dilutions, sources and tissues used for each antibody.

Primary Antibody	Source	Working Dilution	Tissue	Secondary Antibody	Source	Working Dilution
P2X2	Alomone Labs, Jerusalem, Israel	1:600; IHC 1:700; IHC 1:200; WB	U, D Spinal cord Bladder	Cy3-goat anti-rabbit; goat anti-rabbit HRP	Jackson Immunoresearch Laboratories, Inc., West Grove, PA	1:500; 1:500; 1:5K
P2X3	Chemicon International Inc., Temecula, CA	1:700; IHC	U, D	Cy3-donkey anti-guinea pig	Jackson Immunoresearch Laboratories, Inc., West Grove, PA	1:500
P2X3	Neuromics Antibodies, Northfield, MN	1 :650; WB	Bladder	Goat anti-rabbit HRP	Jackson Immunoresearch Laboratories, Inc., West Grove, PA	1:25K
P2X3	Alomone Labs, Jerusalem, Israel	1:700; IHC	Spinal cord	Cy3-goat anti-rabbit	Jackson Immunoresearch Laboratories, Inc., West Grove, PA	1:500
nNOS	Santa Cruz Biotechnology, Inc. Santa Cruz, CA	1:100; IHC	Spinal cord	Cy2-goat anti-mouse	Jackson Immunoresearch Laboratories, Inc., West Grove, PA	1:50
S-100	Dako Cytomation, Norden A/S, Denmark	1:200; IHC 1:400; IHC	Spinal cord	Cy3-goat anti-rabbit	Jackson Immunoresearch Laboratories, Inc., West Grove, PA	1:500
GFAP	Sigma-Genosys, The Woodlands, TX	1:5K;IHC	Spinal cord	Cy2-goat anti-mouse	Jackson Immunoresearch Laboratories, Inc., West Grove, PA	1:100
HuC/D	Molecular Probes, Inc., Eugene, OR	1:200; IHC	Spinal cord	Cy2-goat anti-mouse	Jackson Immunoresearch Laboratories, Inc., West Grove, PA	1:100
PGP9.5	Abcam, Inc., Cambridge, MA	1:15; IHC	U, D	Cy2-goat anti-mouse	Jackson Immunoresearch Laboratories, Inc., West Grove, PA	1:100